GLIA 38:313–328 (2002)

Proteasome Dynamics During Cell Cycle in Rat Schwann Cells

MIGUEL LAFARGA,[1] ROSARIO FERNÁNDEZ,[2] ISABEL MAYO,[3] MARíA T. BERCIANO,[1] AND JOSÉ G. CASTAÑO[3]*

[1]*Departamento de Anatomia y Biología Celular, Universidad de Cantabria, Santander, Spain*
[2]*Departamento de Fisiologia y Farmacología, Universidad de Cantabria, Santander, Spain*
[3]*Instituto de Investigaciones Biomédicas Alberto Sols, CSIC-UAM, Facultad de Medicina, Universidad Autónoma de Madrid, Madrid, Spain*

KEY WORDS proteasome; cell cycle; proteolysis; cytoskeleton; DNA synthesis

ABSTRACT The proteasome is responsible for most of the protein degradation that takes place in the cytoplasm and nucleus. Immunofluorescence and electron microscopy are used to study proteasome dynamics during the cell cycle in rat Schwann cells. During interphase, the proteasome is present in the nucleus and cytoplasm and shows no colocalization with cytoskeletal components. Some cytoplasmic proteasomes always localize in the centrosome both in interphase and in mitotic cells and only associate with microtubules during mitosis. The proteasome exits the nucleus during prophase. In anaphase, the proteasome becomes prominent in the region between the two sets of migrating chromosomes and in association with interzonal microtubules and stem bodies. In telophase, the proteasome begins to reenter the nucleus and is prominent in the midbody region until the end of cytokinesis. The proteasome does not colocalize with actin or vimentin during mitosis, except for colocalization with actin in the sheet-like lamellipodia, which serve as substrate attachments for the cell during mitosis. During S phase, nuclear proteasomes colocalize with foci of BrdU incorporation, but this association changes with time: maximal at early S phase and declining as S phase progresses to the end. These results are discussed in relation to the biochemical pathways involved in cell cycle progression. *GLIA 38:313–328, 2002.*

INTRODUCTION

Cell cycle progression involves a complex spatiotemporal combination of processes driven by changes in gene transcription, protein synthesis, protein localization, and posttranslational modification of proteins: reversible phosphorylation-dephosphorylation, and irreversible proteolysis (Nurse, 2000). Intracellular protein degradation could contribute to the irreversibility of cell cycle transitions, or it could be necessary to change the activities of complexes or protein machines important in cycle progression (Nurse, 2000). Proteins subject to regulated degradation include cyclins and cyclin-dependent kinase inhibitors, tumor suppressors, transcription factors, and cell surface receptors. The ubiquitin-proteasome pathway (Tyers and Jorgensen, 2000) largely accomplishes this protein degradation. Degradation by this pathway requires the covalent attachment of polyubiquitin to proteins, as well as cleavage by proteasomes (Hershko and Ciechanover, 1998). Proteasomes are large multisubunit proteases (20S) composed of four heptameric rings in the configuration $\alpha7\beta7\beta7\alpha7$. These cylindrical particles have their active sites on the inner walls of a central cavity formed by the β-subunit rings (Bochtler et al., 1999). To both α-ring ends of this core 20S proteasome, two ATP-

Grant sponsor: Comisión Interministerial de Ciencia y Tecnología; Grant sponsor: Comunidad Autónoma de Madrid (CAM); Grant number: SAF99-0056; Grant sponsor: CAM and Fundación La Caixa; Grant sponsor: Fondo de Investigaciones Sanitarias; Grant number: 00/0947; Grant sponsor: Fundación Marqués de Valdecilla.

*Correspondence to: José G. Castaño, Departamento de Bioquímica e Instituto de Investigaciones Biomédicas Alberto Sols, UAM-CSIC, Facultad de Medicina, Universidad Autónoma de Madrid 28029, Madrid, Spain.
E-mail: joseg.castano@uam.es

Received 6 November 2001; Accepted 13 February 2002

DOI 10.1002/glia.10075

dependent 19S caps are believed to be attached, forming a 26S proteasome complex. The functions of these 19S caps would be to recognize ubiquitylated protein substrates, to unfold those substrates, and to feed them to the actual protease, the core 20S proteasome (Voges et al., 1999).

Proteasomes in interphase cells are localized in both the nucleus and cytoplasm (Rivett et al., 1992; Arizti et al., 1993; Mengual et al., 1996). More recently, proteasomes were described to be associated with centrosomes in interphase cells (Wigley et al., 1999; Fabunmi et al., 2000). In mitosis, some investigators (Amsterdam et al., 1993; Wojcik et al., 1995) found colocalization of proteasomes with spindle microtubules during metaphase and anaphase; others (Palmer et al., 1996) found proteasomes around chromosomes in metaphase and associated with intermediate filaments (keratin-type) in interphase. Other workers found an association between proteasomes and several cytoskeletal components in interphase cells (Olink-Coux et al., 1994; Arcangeletti et al., 1997, 2000; Foucrier et al., 2001). In contrast, using live fluorescence studies with a fusion protein of subunit LMP2 (interferon-γ [IFN-γ)-inducible β-subunit) and GFP, Reits et al. (1997) concluded that (1) proteasomes are free (i.e., not associated with cytoskeletal components or immobilized on membranes) within the cytoplasm and nucleus in interphase (throughout the cell during metaphase and anaphase), and (2) proteasomes only interchange freely between nucleus and cytoplasm after nuclear envelope breakdown in mitosis. Two major events of the cell cycle, the S and M phase, are associated with selective protein degradation (Tyers and Jorgensen, 2000). A clear picture of the localization of proteasomes during cell cycle is needed.

We selected Schwann cells (SC) to study proteasome localization, as insights into the mechanisms that control SC growth could have practical consequences in nerve regeneration (Goldberg and Barres, 2000); this investigation was a continuation of our previous work on proteasome localization in the central nervous system (CNS) (Mengual et al., 1996). This work presents a comprehensive study of the localization of proteasome with respect to cytoskeleton during interphase and M phase. We also analyze the timing of the exit (prophase) and entry (telophase and cytokinesis) of proteasomes from the nucleus; we report, for the first time, the presence of proteasomes in chromatin regions engaged in active DNA replication during S phase.

MATERIALS AND METHODS

Primary Cultures of Schwann Cells

Sciatic nerves were dissected from 3-day-old Sprague-Dawley rats. SC cultures were prepared as described by (Brockes et al., 1979) and maintained in DMEM supplemented with 10% fetal bovine serum (FBS) for 24 h. Then, cytosine arabinoside 10 μM was added to the culture medium and maintained for 48 h to obtain highly purified SC cultures. On the fourth day, SCs were plated in poly-L-lysine-coated coverslips (Morgan et al., 1991) and maintained for 3 days in 1:1 DMEM/F12 medium supplemented with 10% FBS, 2 μM forskolin, and 20 μg/ml bovine pituitary extract. For S phase studies, growing SC cells were pulsed for 20 min with bromodeoxyuridine (BrdU) at a final concentration of 25 μM and were chased with complete medium without BrdU.

Antibodies

We used rabbit polyclonal antibodies directed against the whole 20S-proteasome complex and subunits C2 (α) and C5 (β) at 1:150 to 1:300 dilution. These antibodies were previously characterized (Mengual et al., 1996; Arribas et al., 1994; Rodriguez-Vilarino et al., 2000). In studying the localization of the 19S proteasome regulatory complex, we used rabbit polyclonal anti-Tbp7 antibodies from Affiniti-Research (UK) at 1:200 dilution. In addition, monoclonal antibodies against β-tubulin (Amersham Life Sciences, The Netherlands; diluted 1:100), pan-actin (clone 4, Roche, Germany; diluted 1:100), vimentin (clone V9, Roche, Germany; diluted 1:15) were used in experiments aimed to study the relationship of proteasome localization and cytoskeleton. Mouse monoclonal anti-nuclear pore complex antibody (clone MAb414, BabCO, Richmond, CA; diluted 1:5,000) was used for double immunofluorescence experiments, to study changes in the nuclear localization of proteasomes. For studies of S phase, we used an anti-BrdU monoclonal antibody (RPN 202; Amersham Life Sciences, The Netherlands) as recommended by the manufacturer.

Immunofluorescence

SCs grown in coverslips were washed twice in phosphate-buffered saline (PBS) and were fixed with 3.7% paraformaldehyde in PBS (20 mM Na Pi, pH 7.4, 0.14 M NaCl) for 15 min at room temperature. Cells were permeabilized with 0.5% Triton X-100 for 30 min and were treated with 0.1 M glycine in PBS for 45 min. Alternatively, the cells were fixed in methanol for 10 min at −20°C.

For immunofluorescence studies, SCs fixed with paraformaldehyde or methanol were washed in PBS containing 0.01% Tween 20 for 5 min and incubated with the primary antibodies diluted in PBS for 1 h at room temperature. For double-labeling experiments, the two primary antibodies were incubated sequentially (1 h each). Antibody-binding sites were detected with secondary antibodies conjugated to either fluorescein isothiocyanate (FITC) or Texas Red (TxRed) (Jackson Laboratories, USA). The coverslips were mounted with the antifading medium Vectashield (Vector, USA). Samples were examined with a confocal microscope (Bio-Rad MRC-1024) using argon ion (488-nm) and HeNe (543-nm) lasers to excite FITC and TxRed, re-

spectively. For double-labeling experiments, images from the same confocal plane were sequentially recorded and superimposed. Controls with pre-immune sera or secondary antibodies alone were all negative by immunofluorescence.

Immunoelectron Microscopy

For immunoelectron microscopy, SCs were fixed with 4% paraformaldehyde in 0.1 M cacodylate buffer for 1 h at room temperature. The cells were scraped from the dishes, transferred to an Eppendorf tube, and centrifuged for 1 min in a microfuge, to pellet the cell cultures. The pellets were washed with 0.1 M cacodylate buffer, dehydrated in increasing concentrations of methanol at −20°C, embedded in Lowicryl K4M at −20°C, and polymerized with ultraviolet (UV) irradiation. Ultrathin sections were mounted on nickel grids and sequentially incubated with 0.1 M glycine in PBS for 15 min, 5% BSA in PBS for 1 h, and the anti-proteasome antibody (diluted 1:50 in PBS containing 1% BSA and 0.1 M glycine) for 1 h. After washing, the sections were incubated with goat anti-rabbit IgG coupled to 5-nm or 10-nm gold particles (BioCell, UK; diluted 1:50 in PBS containing 1% BSA). For double immunoelectron microscopy, samples of SCs pulse-labeled with BrdU were fixed in paraformaldehyde and embedded in Lowicryl K4M as indicated above. Ultrathin sections mounted on nickel grids were incubated sequentially with anti-BrdU monoclonal antibody (diluted in 50 mM Tris-HCl, pH 7.6, containing 1% BSA and 0.1 M glycine) for 14 h at 4°C; with goat anti-mouse IgG conjugated with 6-nm colloidal gold particles (Aurion, Belgium) diluted 1:20 in 0.02 M Tris-HCl, pH 8.2, containing 1% BSA for 1 h at room temperature; with rabbit anti-proteasome antibody (diluted 1:50 in PBS containing 1% BSA and 0.1 M glycine); and with goat anti-rabbit IgG coupled with 15-nm gold particles (BioCell, UK, diluted 1:50 in PBS containing 1% BSA) for 1 h at room temperature. After immunogold labeling, the grids were stained with lead citrate and uranyl acetate and were examined with a Philips EM208 electron microscope operated at 60 kV. As controls, ultrathin sections were treated as described above with pre-immune sera from rabbit or mouse or omitting primary antibodies, no immunogold labeling was obtained under those conditions.

RESULTS

Proteasome Localization During Interphase and Mitosis With Relation to the Cytoskeleton

We have analyzed the distribution of proteasomes by double labeling experiments using anti-proteasome antibodies in combination with antibodies against tubulin (microtubules), actin (microfilaments), and vimentin (intermediate filaments) in SCs (Mirsky and Jessen, 1999). The aim was to study the possible association of proteasomes with the cytoskeletal network whose dynamics are critical during mitosis. Figure 1A shows a typical distribution of proteasomes in interphase SCs. Proteasome is present in both the nucleus and cytoplasm, as expected. Within the nucleus, the proteasome appears widespread throughout the nucleoplasm, with some brighter dots, whereas the nucleolus and the peripheral rim of heterochromatin attached to the nuclear envelope are not stained. In the cytoplasm, a similar diffuse distribution with some dots of higher staining intensity can be observed. By double staining with anti-proteasome and anti-tubulin antibodies (Fig. 1B, merged Fig. 1C), no association between the proteasome and the microtubule network can be detected, except for the strong colocalization within the centrosome.

In early prophase (Fig. 1D–F), chromosome condensation occurs, and duplicated centrosomes move along the nuclear envelope in the SCs. At this mitotic stage, proteasome staining in the nucleus begins to disappear from the chromosomal territories, and the remaining labeling appears localized to the nucleoplasmic interstices among the condensing chromosomes. In the cytoplasm proteasome, immunofluorescence shows a diffuse distribution with a clear increase at the centrosomes. By late prophase (Fig. 1G–I), proteasome immunofluorescence was completely absent from the nucleus and, within the cytoplasm, it is prominent at the two centrosomes. At metaphase, the proteasome signal was heavily concentrated in the punctate centrosomes, with some detected along the polar and kinetochore microtubules, but it is absent from the astral microtubules (Fig. 1J–L). During early anaphase, proteasome immunofluorescence is located at the centrosomes, along the polar and kinetochoric microtubules, and in the mid-zone region between the separating daughter chromosomes (Fig. 2A–C). By late anaphase, when the chromosomes have almost reached the opposite spindle poles, proteasome immunofluorescence appears strongly concentrated in the centrosome, and in association with the interzonal microtubules and stem bodies (Fig. 2D–F). At late telophase, proteasomes are concentrated in the cytoplasmic midbody and begin to reappear inside the reassembled nuclei (Fig. 2G–I). As the telophase ends and cytokinesis begins, proteasome immunofluorescence is clearly observed in the nuclei of the two separating cells, and a brilliant focus of proteasome immunostaining is observed in the slender connecting bridge between the separating daughter cells (Fig. 2J–L). In addition, sheet-like lamellipodia, which are thought to exert tension to separate the daughter cells, were commonly immunostained for proteasomes during telophase and cytokinesis (see below). Note that the proteasome is also localized during telophase and cytokinesis in the centrosome of the two separated cells (see arrows, Fig. 2I,L); its less prominent appearance is attributable to focusing at the plane of separation of the two round sister cells.

The relationship of proteasome localization with respect to actin (microfilaments) and vimentin (interme-

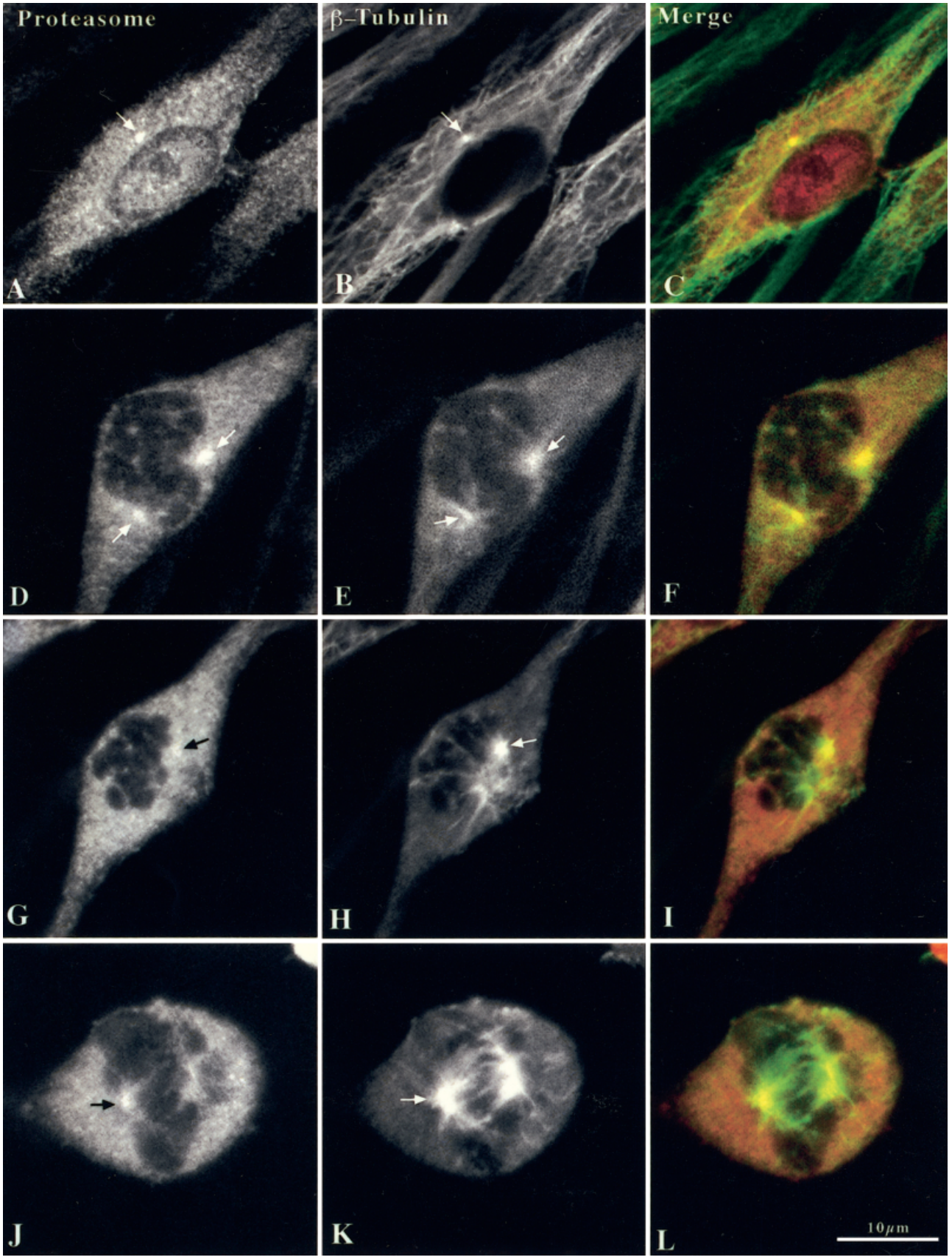

Fig. 1. Localization of proteasomes with respect to microtubules during interphase and mitosis in Schwann cells. Double immunofluorescence experiments with anti-whole proteasome (red) and anti-β-tubulin (green) antibodies. Interphase (**A,B**, and merge **C**). Early prophase (**D,E**, and merge **F**). Late prophase (**G,H** and merge *I*). Metaphase (**J,K** and merge **L**). Arrows point to centrosomes.

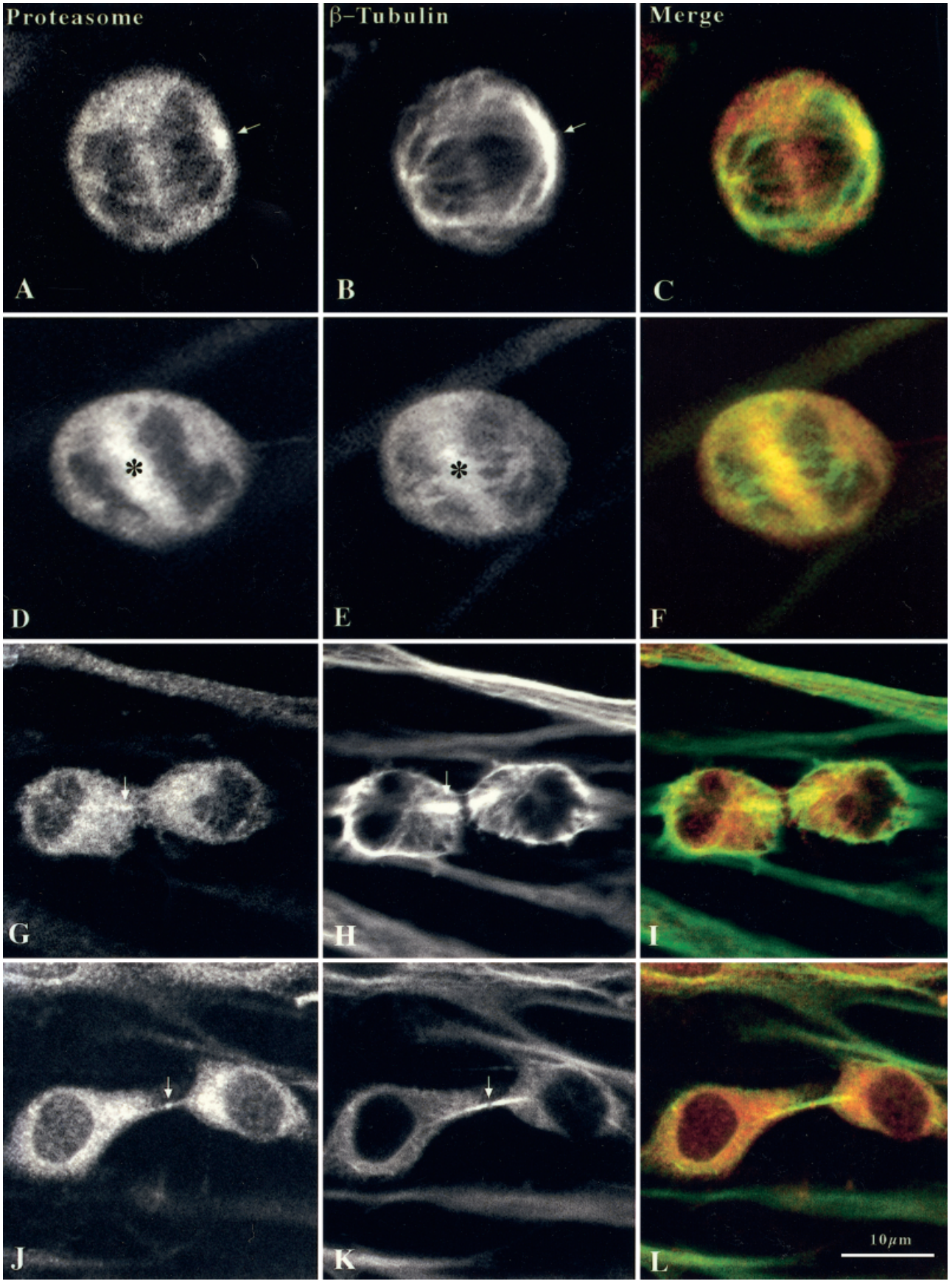

Fig. 2. Localization of proteasomes with respect to microtubules during mitosis in Schwann cells. Double immunofluorescence with the anti-whole proteasome (red staining) and anti-β-tubulin (green staining) antibodies. In early anaphase, a prominent centrosome (arrow) is shown in this plane immunostained with the anti-whole proteasome antibody (**A,B**, and merge **C**). **D,E**, and merge **F:** late anaphase showing a high concentration of proteasomes (asterisks) at the interchromosomal mid-region. **G,H**, and merge **I:** telophase illustrating the accumulation of proteasome (arrows) at the interzonal. During late telophase proteasome staining reappears in the cell nucleus (**J,K**, and merge **L**). Note the concentration of proteasome at the mid-body (arrows) of the intercellular bridge during cytokinesis.

diate filaments) was subsequently explored. Actin organization in SC cells during interphase (Fig. 3B) shows the typical distribution pattern, with long bright bundles along the main axis of the cell (Weiner et al., 2001). Double-labeling experiments using anti-actin and anti-proteasome antibodies demonstrate no colocalization of actin cytoskeleton with proteasomes (Fig. 3A). Similarly, at metaphase and anaphase, proteasome distribution (Fig. 3C) does not colocalize with the actin-rich cell cortex of SC (Fig. 3C,D). Proteasome immunostaining was also absent in the cortical actin domains of the cleavage furrow and in the contractile ring during telophase and cytokinesis (Fig. 3E–H). Noteworthy is the presence of a bright spot of proteasome staining between the actin rings at the midbody region. There is a clear exception to the general conclusion that actin cytoskeleton and proteasome do not colocalize in both interphase and mitotic SCs: actin and proteasome colocalize in the actin-rich cortical domains involved in the formation of blebs or sheet-like lamellipodia. These two dynamic structures are assembled and disassembled to increase and release tension, respectively, in regions of substrate cell adhesion, especially during cytokinesis. Note that tubulin and vimentin (Fig. 3; and see below) are absent from these membrane blebs.

Similar double immunofluorescence studies with proteasomes and the major intermediate filament protein in the SCs, i.e., vimentin, show no colocalization of immunolabeling with the two antibodies in either the interphase cells (Fig. 3I,J), in which vimentin shows the characteristic bundles of filaments, or the mitotic cells (Fig. 3K–N), in which the vimentin signal is diffusely distributed at the cell periphery and excluded from cell sites enriched in proteasome signal, such as mitotic spindles and the interchromosomal mid-zone region.

The proteasomal distribution during mitosis (see above) is independent of the method of cell fixation, whether methanol or formaldehyde. Furthermore, almost identical distribution was observed when proteasome localization was performed with antibodies specific for single subunits of the proteasome. As shown in Figure 4, polyclonal antibodies directed against single proteasomal subunits: C2 (α-subunit, Fig. 4A,D,G,J) and C5 (β-subunit, Fig. 4B,E,H,K) gave a strong immunofluorescence signal in the same intracellular locations as those described above with the anti-whole proteasome antibodies. The reduced level of nuclear staining in interphase with the subunit-specific antibodies (almost absent in the case of the anti-C5 antibody), compared with whole proteasome antibody staining, is probably attributable to masking of epitopes recognized by these antibodies in the nuclear proteasome population (Arribas et al., 1994; Rodriguez-Vilarino et al., 2000). As the 20S proteasome forms a complex with the 19S regulator to form the 26S–proteasome complex (Voges et al., 1999), it was interesting to demonstrate whether a similar distribution of the 19S cap could be observed during mitosis. To that end,

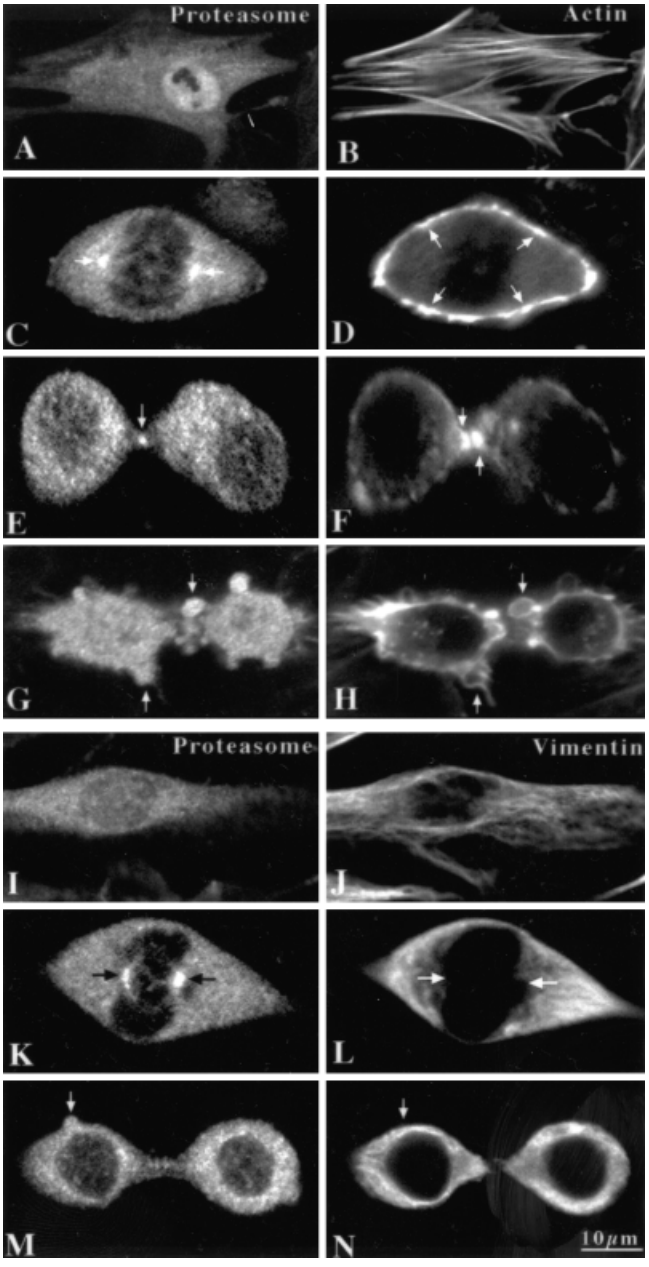

Fig. 3. Localization of proteasomes with respect to microfilaments and intermediate filaments during interphase and mitosis in Schwann cells. Double immunofluorescence with anti-whole proteasome and anti-actin, or anti-vimentin antibodies. Interphase: actin (**A,B**); vimentin (**I,J**). Metaphase: actin (**C,D**), vimentin (**K,L**). Late telophase: actin (**E,F**) and vimentin (**M,N**). Cytokinesis: actin (**G,H**). During interphase (A,B) actin staining is prominent in stress fibers, no colocalization with anti-proteasome staining. At metaphase, proteasome is particularly concentrated at centrosomes (C, arrows), while actin staining is mainly distributed at the cell cortex (D, arrows). During telophase, a focal accumulation of proteasome is visible at the mid-body (E, arrow), whereas the contractile ring of the intercellular bridge shows a prominent actin staining (F, arrows). In cytokinesis proteasome and cortical actin colocalize in the blebs or sheet-like lamellipodia (G,H, arrows) formed by the cell membrane of daughter cells. No clear colocalization was observed in double staining with anti-proteasome and anti-vimentin (**I–N**).

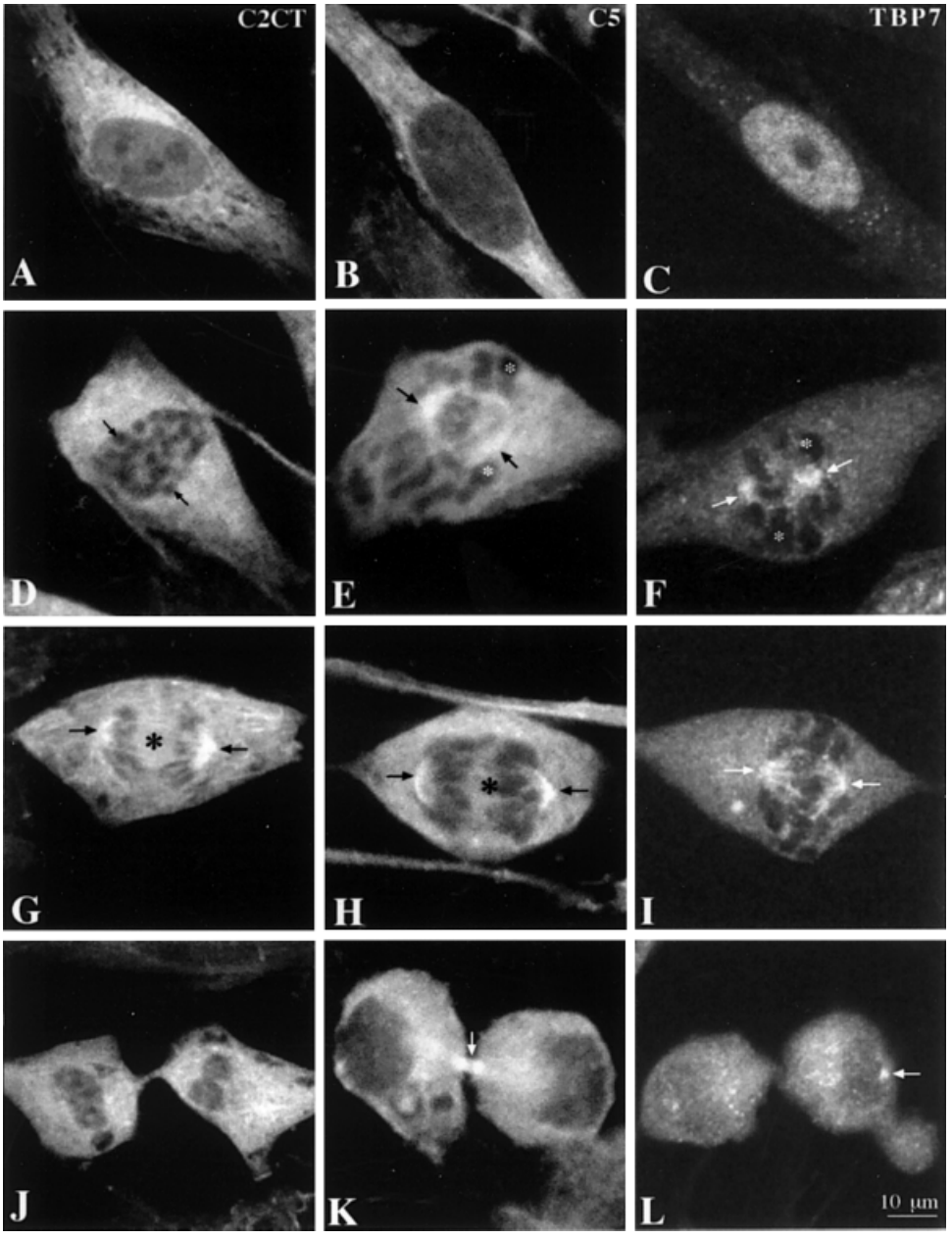

Fig. 4. Localization of proteasomes with antibodies specific for proteasomal subunits of the 20S complex and with an anti-Tbp7 antibody (a subunit of the 19S regulatory complex) in interphase cells and mitosis. Anti-C2 antibody staining is observed in the cytoplasm and cell nucleus, excluding the nucleolus, of a interphase Schwann cell (**A**), in the nucleoplasmic domains among condensing chromosomes (arrows) in prophase (**D**), in centrosomes (arrows) and in the interchromosomal mid-region (asterisk) in anaphase (**G**), and in the cytoplasm and cell nucleus at the late telophase (**J**). Anti-C5 antibody exhibits little immunostaining of the cell nucleus in interphase (**B**); immunostaining is present in centrosomes (black arrows) and absent from condensing chromosomal domains (asterisks) in prophase (**E**); in anaphase the staining is concentrated in centrosomes and in the mid-region (**H**, black arrows and asterisk, respectively) and in telophase is concentrated in the interzonal region (**K**, white arrow). Anti-Tbp7 antibody staining is concentrated in the cell nucleus, excluding the nucleolus, during interphase (**C**) and in centrosomes (white arrows) in prometaphase (**F**), metaphase (**I**), and telophase (**L**) cells. Note the absence of immunolabeling in the condensing chromosome domains of the prometaphase (**F**).

we used polyclonal antibodies directed against one of the subunits of the base of the 19S-regulator complex, Tbp7. The results obtained (Fig. 4C,F,I,L) are similar to those described with the anti-20S proteasome antibodies (cf. Figs. 1, 2, 4) and with anti-subunit specific antibodies (also shown in Fig. 4). These results illustrate that a part of the cellular 19S complex behaves like the 20S proteasome catalytic core during interphase and mitosis, whereas they apparently colocalize only partially (see Discussion).

To demonstrate further the subcellular structures to which proteasomes are associated during mitosis, we performed immunoelectron microscopic localization, using the anti-whole proteasome antibody. Labeling of

control sections with pre-immune sera or secondary antibody was negligible. The results in Figure 5 are representative of at least 20 SCs for each of the mitotic stages depicted. Figure 5A shows the localization of proteasomes within the centrosome of a cell in metaphase; the immunogold particles were found over the pericentriolar matrix and also decorated the adjacent cytoplasmic area of distribution of polar and kinetochore microtubules around the chromosomes. Furthermore, during anaphase, immunogold particles were concentrated in a mid-zone equatorial region of the cell between separating daughter chromosomes of a cell in anaphase. Finally, Figure 5C illustrates the distribution of proteasome immunogold particles in a bleb of the plasma membrane of a cell in telophase. These results illustrate the major findings of proteasome localization during mitosis by confocal immunofluorescence microscopy at the ultrastructural level.

Nuclear Export and Import of Proteasomes During Mitosis

The changes that occur in the nuclear contents of proteasome during mitosis are described above. Because this process is a key mechanism for the control of the activity of many proteins participating in cell cycle regulation, we have performed a detailed analysis of nuclear exit and entry of proteasomes during mitosis. In early prophase, the level of proteasomal staining within the nucleus is reduced, with respect to interphase SCs (Fig. 6A). During prometaphase (Fig. 6B), nuclear staining of the proteasome decreases, and the cytoplasmic proteasome becomes quite prominent at separating centrosomes (as described above). To obtain further evidence, double immunofluorescence experiments were carried out with anti-proteasome and with a monoclonal antibody against the nuclear pore complex (NPC). Figure 6E,F clearly demonstrates that redistribution of the proteasome is initiated during prophase (Fig. 6E), when the nuclear envelope is totally preserved (Fig. 6F) and the delineation of condensed chromosomes free of anti-proteasome staining during prometaphase (Fig. 6G) is associated with total disassembly of the nuclear envelope (Fig. 6H). These results clearly suggest that the nuclear export of proteasome begins during early prophase, when the nuclear envelope is still intact and goes in parallel with chromosome condensation.

Proteasome entry into the cell nucleus takes place during late telophase and cytokinesis and after the two daughter cells have separated. Figure 6C shows an early telophase, in which proteasome staining is distributed through the cytoplasm, with a strong concentration at the centrosomes and in the region in which the cleavage furrow is beginning to separate the two cells. By late telophase, when nuclear envelope is fully reassembled (Fig. 6D), proteasome immunofluorescence begin to appear inside the nucleus (note that chromosomal decondensation is almost complete). Again, to demonstrate further the dynamics of proteasome translocation, we performed double immunofluorescence studies with anti-proteasome and anti-NPC monoclonal antibody. In early telophase, the proteasome is located almost exclusively in the cytoplasm (Fig. 6I), and the nuclear envelope is almost completely re-formed (Fig. 6J). During late telophase, the proteasome begins to reappear in the cell nucleus (Fig. 6K), and the nuclear envelope is completely assembled (Fig. 6L). These results clearly suggest that the nuclear import of the proteasome is initiated during late telophase, when the nuclear envelope is almost fully reconstituted, and appears to go in parallel with chromosome decondensation.

To demonstrate further the changes in nuclear proteasomes during prophase and telophase, we also performed immunoelectron microscopic studies for proteasome localization. Figure 7A,B depicts representative immunogold labeling of prophase cells; controls with pre-immune sera or secondary antibodies were negative. Proteasome immunogold particles were associated with dispersed chromatin domains among condensed chromatin masses, with the nucleoplasmic border of heterochromatin and with the nuclear envelope. Gold particles were conspicuously absent in the heterochromatin regions. In addition, clusters of gold particles decorated small nuclear microdomains composed of dense material that appeared scattered through the nucleoplasm. During the re-formation of daughter cell nuclei in telophase, gold particles of proteasome immunoreactivity reappeared in the cell nucleus (Fig. 7B). They specifically labeled both electrolucent nucleoplasmic areas of variable size that were localized among decondensing chromosomes as well as the narrow nucleoplasmic interstices created by the unfolding of chromatin fibers. Some immunogold particles also appeared in the reassembled nuclear envelope. These results illustrate the results obtained with confocal immunofluorescence microsocopy at a higher resolution (i.e., the ultrastructural level).

Dynamics of Proteasome During the S Phase of the Cell Cycle

One advantage of using primary culture SC cells is that they can be easily synchronized by serum starvation. Their entrance into the cycle is promoted by the addition of forskolin, serum, and pituitary extract, which produce a culture in which approximately 40% of cells enter synchronously in S phase, as judged by the incorporation 5-bromodeoxyuridine (data not shown). We performed double immunofluorescence experiments with anti-BrdU and anti-proteasome antibodies of SC cells that received a pulse with BrdU for 20 min and were washed and then followed for the next 4 h. Figure 8 shows the representative results obtained at three stages of S phase. In early S phase, when DNA replication localizes mainly in dispersed chromatin domains all over the nuclear interior (Hozak et al., 1994; Mazzotti et al., 1998; Wei et al., 1998), proteasome

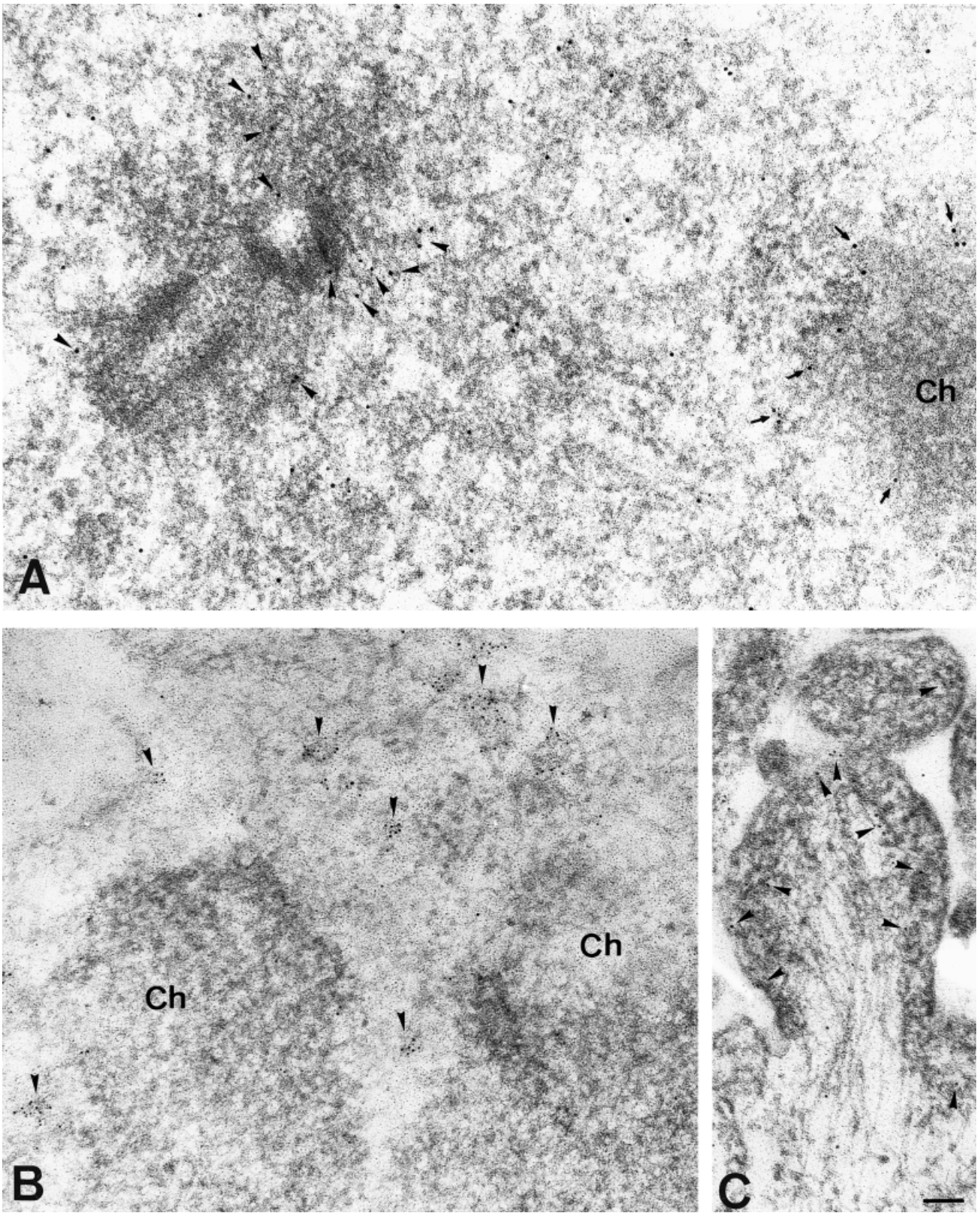

Fig. 5. Immunoelectron microscopy distribution of proteasome in mitotic Schwann cells. **A:** Spindle pole of a metaphase showing a prominent centrosome with a pair of centrioles. Immunogold particles for proteasome mainly decorated the pericentriolar matrix (arrowheads). Some particles extend away from the centrosome in the area of distribution of the kinetochoric and polar microtubules. Note the presence of proteasome labeling at the edge of a chromosome (arrows). **B:** Anaphase illustrating the mid-equatorial zone between separating daughter chromosomes (Ch). Several clusters of gold particles for proteasome are visible in this region (arrowheads). **C:** Detail of a lamellipodium of a Schwann cell in telophase. Note the axial cytoskeleton of microfilaments and the presence of proteasome gold particles at the cell cortex of this lamellipodium (arrowheads). Scale bars = 0.1 μm in A,B,C.

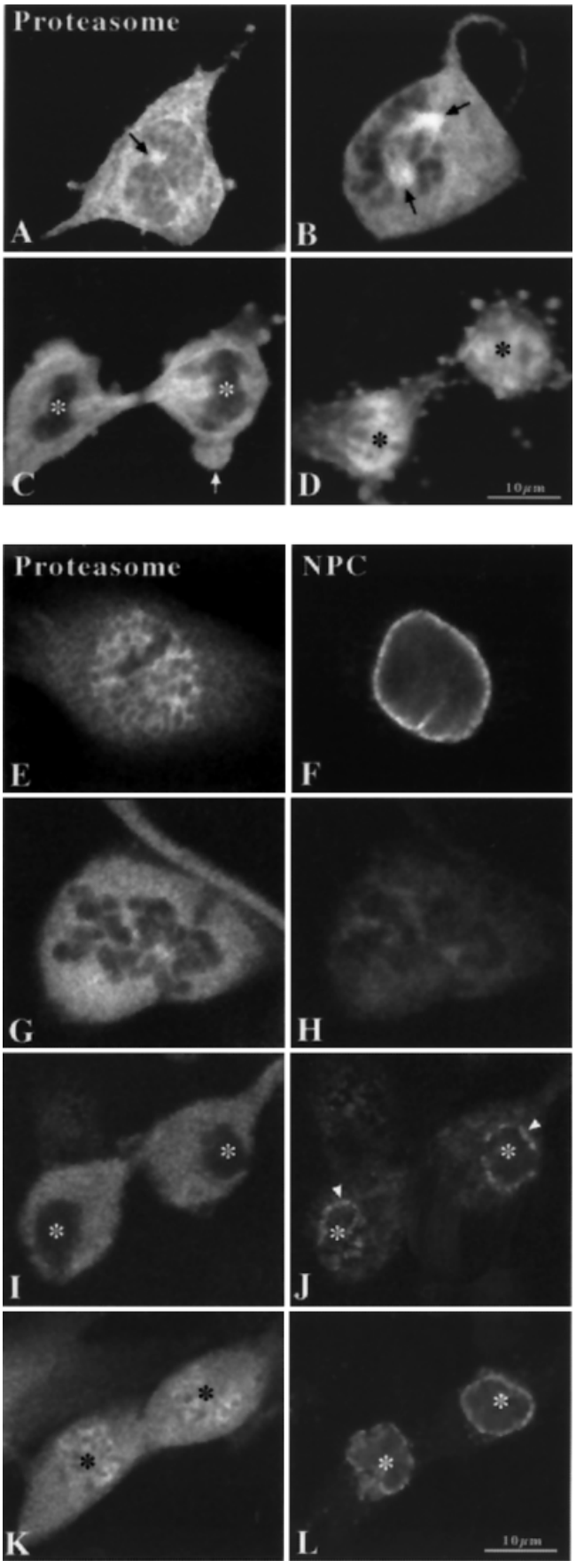

immunostaining exhibited a diffuse nucleoplasmic pattern with some small foci (Fig. 8A). BrdU incorporation also showed a diffuse nucleoplasmic staining in addition to small foci (Fig. 8B). Most important, superposition of the two images shows that proteasome colocalizes with BrdU for most part of the nuclear foci (Fig. 8C). By mid-S phase, when BrdU incorporation appears to be associated mostly with the border of heterochromatin clumps at the nuclear and nucleolar periphery (Hozak et al., 1994; Mazzotti et al., 1998; Wei et al., 1998), the colocalization of proteasome and BrdU foci shows minor changes with respect to early S phase (Fig. 8D–F). Late S phase is characterized by the presence of large clusters of BrdU incorporation, concurring with masses of heterochromatin at the nuclear periphery, as illustrated in Figure 8H, and as previously demonstrated (Hozak et al., 1994; Mazzotti et al., 1998; Wei et al., 1998). At this stage, there is little colocalization of BrdU and proteasome clusters (Fig. 8G–I). Similar results were obtained with anti-Tbp7 antibody (data not shown), indicating that not only the 20S proteasome catalytic core, but also the 19S proteasome regulatory complex, is present at chromosomal regions in which BrdU incorporation takes place during S phase.

To demonstrate the actual colocalization of proteasome and regions of BrdU incorporation during S phase, we performed double immunogold staining with anti-BrdU and anti-proteasome antibodies; controls with rabbit and mouse pre-immune sera were negative. Figure 9 shows a representative nucleus of a cell at mid-S phase; some gold particles of BrdU clearly colocalize with gold proteasome particles in small nuclear foci, whereas others do not colocalize. Colocalization of BrdU and proteasome is observed only on the dispersed chromatin, but not on the peripheral masses of heterochromatin; this ultrastructural image is fully compatible with observations by confocal microscopy.

Fig. 6. Nuclear exit and reentry of proteasomes during mitosis. **A–D:** Simple immunofluorescence with the anti-whole proteasome antibody. In early prophase, nuclear proteasome is distributed in the narrow nucleoplasmic interstices among condensing chromosomes, at the nuclear envelope and in the centrosome (A, black arrow). During prometaphase, condensed chromosome domains are free of immunostaining, while a strong staining is observed at the centrosomes (B, black arrows). In early telophase proteasome immunoreactivity is absent from the cell nucleus (C, white asterisks) and reappears during late telophase (D, black asterisks). **E–L:** Double immunofluorescence experiments with the anti-whole proteasome and the anti-nuclear pore complex (NPC) antibodies. Redistribution of proteasome initiates during prophase, when the nuclear envelope is completely preserved (**E,F**). The complete delineation of condensed chromosome domains free of proteasome immunostaining during prometaphase (**G**) is associated with total disassembly of the nuclear envelope (**H**). In early telophase (**I,J**) the nuclei of daughter cells show complete absence of proteasome signal (white asterisks), while the nuclear envelope is almost completely reformed (**J**, white arrowheads). During late telophase, proteasome reappears within the cell nuclei (**K**, black asterisks) when the nuclear envelope is completely assembled (**L**, white asterisks).

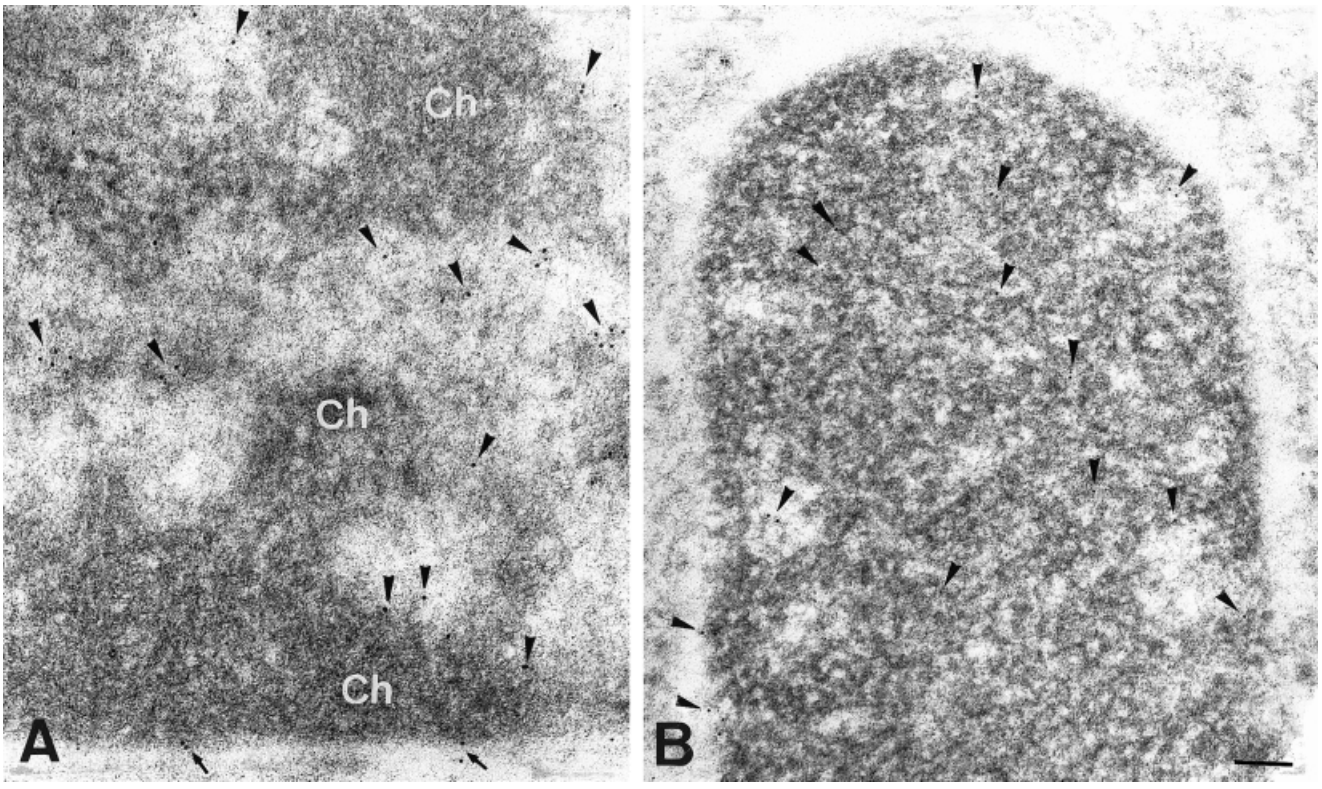

Fig. 7. Nuclear distribution of proteasome in prophase and telophase Schwann cells studied by immunoelectron microscopy. **A:** Prophase Schwann cell showing immunogold particles for proteasome (arrowheads) distributed throughout nuclear interstices of dispersed chromatin among the condensing chromosomes (Ch), which appear free of immunolabeling. Some gold particles are associated with the nuclear envelope (arrows). **B:** Telophase Schwann cell showing reappearance of proteasome in the cell nucleus. Gold particles (arrowheads) are visible on the nucleoplasmic interstices among the dense threads of unfolding chromatin fibers. Scale bar = 0.1 μm in A,B.

DISCUSSION

Cell cycle progression involves a complex spatiotemporal combination of processes orchestrated by the cyclin-dependent protein kinases. Two main biochemical mechanisms, protein phosphorylation-dephosphorylation and proteolysis, have a central role in cell cycle control (Nurse, 2000). Only recently has protein localization warranted more attention as an important mechanism of cell cycle control (LaBaer et al., 1997; Donaldson and Blow, 1999; Cerutti and Simanis, 2000; Muller et al., 2000). Live fluorescence imaging has emerged as the ideal approach to study spatiotemporal changes in protein distribution. However, this technique requires initial validation with conventional indirect immunofluorescence as well as careful interpretation of the results; it can also require ultrastructural confirmation. Detailed conventional immunofluorescence studies combined with electron microscopy are still indispensable tools with which to study protein localization and dynamics in the cell. We have followed the latter approach to study the dynamics of proteasome distribution during cell cycle in SCs. Major findings have also been verified in NRK and HeLa cells.

The results presented are of general application for proteasome localization during the cell cycle in mammalian somatic cells. We have used polyclonal antibodies against the whole 20S proteasome complex; in these studies, no significant differences were obtained when subunit-specific antibodies were used (Figs. 1, 2, 4), except for some changes in nuclear staining in interphase cells. These differences in nuclear staining are attributable to epitope masking in the nuclear proteasome population, and not to differences in the amount of those subunits in the pool of the nuclear proteasome population (Arribas et al., 1994; Rodriguez-Vilarino et al., 2000). Epitope masking may also explain some of the changes reported when immunofluorescence studies are performed with monoclonal antibodies to specific proteasomal subunit (Wojcik et al., 1995). We have also used antibodies against Tbp7, a component of the base of 19S regulatory complexes (Voges et al., 1999), obtaining a similar cellular distribution and dynamics for this complex as for the 20S–proteasome complex. Although we were unable to carry out colocalization studies in rat SCs with anti-proteasome and anti-Tbp7 antibodies, some colocalization has been demonstrated using human cell lines (Wigley et al., 1999). Ours results demonstrate that a part of the cellular 19S complex behaves like the 20S proteasome catalytic core, but this finding does not suggest that all 20S complexes are associated with the 19S complex forming the 26S complex. Initial (Yang et al., 1995) and more recent studies (Brooks et al., 2000; Tanahashi et al., 2000)

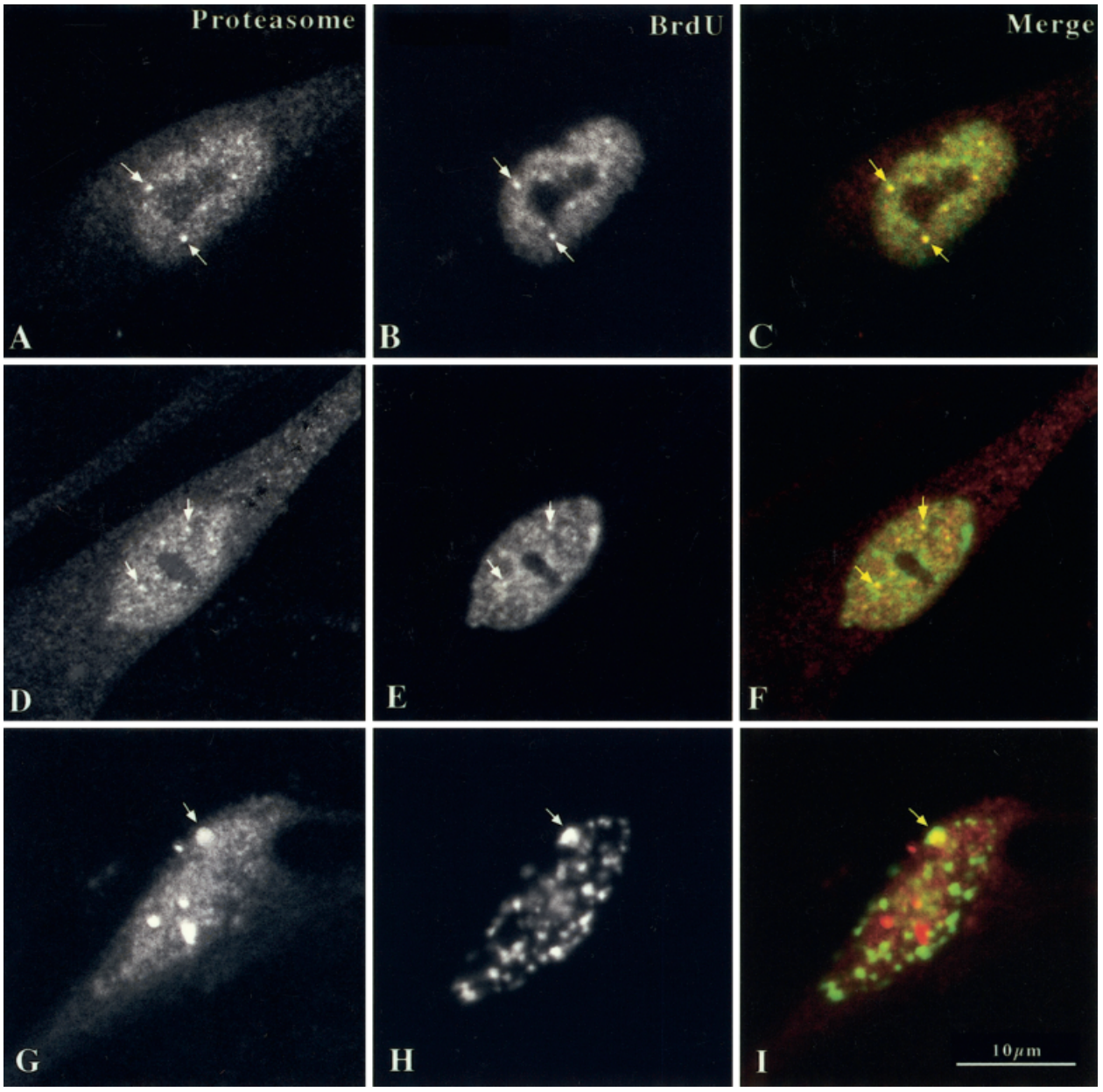

Fig. 8. Nuclear localization of proteasomes during S phase of the cell cycle. Schwann cells were pulse-labeled with BrdU for 20 min and were chased with complete medium without BrdU. Cells were processed for double immunofluorescence analysis with the anti-whole proteasome (red-staining) and anti-BrdU (green-staining) antibodies. Early S phase (**A,B**, and merge **C**). Middle S phase (**D,E**, and merge **F**). Late S phase (**G,H**, and merge *I*). Proteasome and BrdU colocalize in several nuclear foci (arrows) distributed throughout the nucleoplasm.

show that only a fraction of the 20S proteasome is associated with the 19S complex (forming the 26S complex) in the cell, albeit dissociation of the complex during isolation cannot be excluded. The 19S complex, without requirement of the 20S catalytic component, plays a role in DNA excision repair in yeast (Russell et al., 1999; Gillette et al., 2001) and in elongation of RNA pol II transcription (Ferdous et al., 2001). These results support the notion that the function of 19S complex is not limited to the delivery of ubiquitylated proteins to the 20S proteasome for degradation.

The distribution of proteasome in interphase SCs is similar to that reported in other mammalian somatic cells (Rivett et al., 1992; Arizti et al., 1993; Amsterdam et al., 1993; Palmer et al., 1994; Wojcik et al., 1995; Mengual et al., 1996). The proteasome shows a diffuse nuclear and cytoplasmic distribution. Within the nucleus, proteasomes are excluded from the nucleoli and from a peripheral rim, clearly corresponding to the distribution of heterochromatin clumps associated with the nuclear envelope. In interphase, we found no colocalization of proteasomes with the components of cy-

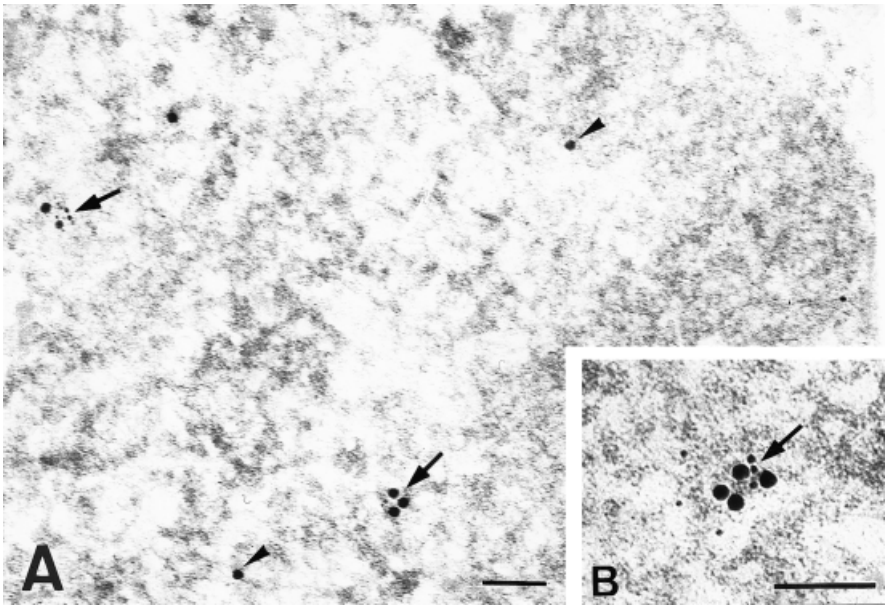

Fig. 9. Electron micrographs of S phase Schwann cells labeled with anti-BrdU and anti-proteasome antibodies. Developing was performed with gold-labeled secondary antibodies, anti-mouse (for anti-BrdU, 6 nm) and anti-rabbit (for anti-proteasome, 15 nm). **A:** Two small cluster containing both BrdU and proteasome gold particles are visible over euchromatin (arrows). Some gold particles for proteasome appear scattered throughout the euchromatin (arrowheads). **B:** High-power view of a cluster of gold particles marking a replication site, in which 6-nm particles of BrdU colocalize with proteasome (15 nm). Scale bar = 0.1μm in A,B.

toskeleton (tubulin, actin, and vimentin) in SCs. These results are in agreement with the proteasome distribution reported by Reits et al. (1997), using live fluorescence imaging with a GFP-LMP2 fusion construct in HT1080 (human fibrosarcoma cell line), although these investigators did not validate their live fluorescence studies with indirect immunofluorescence.

We found proteasome localization in the centrosome, not found in early reports (Rivett et al., 1992; Palmer et al., 1994; Wojcik et al., 1995; Mengual et al., 1996) and reported more recently (Wigley et al., 1999; Fabunmi et al., 2000). Proteasomes also localized along the kinetochoric and polar microtubules during mitosis. Although the presence of proteasomes in centrosomes is a constant finding throughout the cell cycle, the association with microtubules only appears clearly during mitosis. Reits et al. (1997) did not describe the localization of proteasomes in centrosomes (interphase or mitosis) or the microtubule association during mitosis. Using photobleaching experiments, these investigators estimate that only 3% of the nuclear proteasome and 8% of the cytoplasmic proteasome is immobilized. In our opinion, they overinterpret their results by concluding that proteasomes cannot be found accumulated in discrete subcellular localization, arguing that those are artifacts of cell fixation. A guide to interpret these experiments on proteasome localization is the careful (live fluorescence and immunofluorescence) experiments performed by (Phair and Misteli, 2000) on proteins that show localization to discrete nuclear compartments (i.e., splicing factors and nucleolar and nucleosomal binding proteins). These nuclear proteins move as free proteins in the nucleus (i.e., they are not immobilized in the corresponding compartments), and their localization is the reflection of the steady-state association/dissociation with those nuclear compartments.

As a consequence, we can formulate an interpretation that reconciles both data from indirect immunofluorescence and live fluorescence studies on proteasomes. Proteasomes, although free within the nucleus and cytoplasm, show discrete intracellular regions in which their steady-state concentration is higher. Such regions (e.g., centrosome, microtubules, and nuclear and cytoplasmic dots) are not formed by sequestered proteasomes; rather, they are in equilibrium with the rest of the proteasome population within the cytoplasm (or the nucleus). We have also shown that proteasomes do not colocalize with actin and vimentin during mitosis. These results provide another argument in favor of the specificity of the association of proteasomes with microtubules and centrosomes. The exception is proteasome localization with actin in the sheet-like lamellipodia, which help the cell attach to substratum. This association occurs during all steps of mitosis, and especially during telophase and cytokinesis. These sheet-like lamellipodia are highly dynamic structures that rapidly arise and retract in different domains of the cell cortex. Our results clearly suggest that the proteasome may play a role in the assembly-disassembly cycle of these cortical structure processes (Cooper and Schafer, 2000; Goode et al., 2000).

The distribution of proteasomes during mitosis is an indication of regions in which preferential proteolysis might take place. It is noteworthy that cyclin B1 degradation begins at the centrosomes and in the mid-zone region between the chromosomes during anaphase

(Clute and Pines, 1999), precisely the two regions in which proteasome immunofluorescence demonstrates higher steady-state levels. Furthermore, localization of the APC–cyclosome complex (Kurasawa and Todokoro, 1999), responsible for the ubiquitylation of cyclin B (and other proteins during metaphase to anaphase transition), follows a similar distribution as proteasomes, localized in the centrosomes and mitotic spindles throughout mitosis and in the midbody during telophase and cytokinesis. In contrast, the APC–cyclosome complex is also localized in the kinetochores from prophase to anaphase (Jorgensen et al., 1998; Kurasawa and Todokoro, 1999), but this localization is not found for the proteasome. The localization of proteasomes in the centrosome during mitosis may also indicate that proteasomes are implicated in the degradation of proteins that cannot be transported through the secretory pathway due to the disassembly of the endoplasmic reticulum and Golgi complex during mitosis (Zaal et al., 1999; Farmaki et al., 1999; Chao et al., 1999). This physiological situation is similar to the cellular stress induced with the expression of mutant membrane proteins that cannot reach their final destination in the secretory pathway, such as the ΔF508 mutant CFTR that becomes accumulated in the centrosome (Wigley et al., 1999) given rise to the formation of aggresomes (Johnston et al., 1998; Notterpek et al., 1999).

Our results demonstrate, for the first time, the nuclear proteasome dynamics during mitosis. Proteasome export from the nucleus begins in early prophase and is absent from the nucleus in late prophase. The reentry of proteasome into the nucleus begins late in telophase and continues during cytokinesis, when the nuclear envelope has been completely reassembled. These results suggest that proteasome export and import to the nucleus is a regulated process during mitosis. The massive exit of the nuclear proteasome in prophase is coincident with the reported massive entry of cyclin B1 to the nucleus due to inhibition of cyclin B1 export (Clute and Pines, 1999). The reciprocal nuclear translocation of cyclin B1 and proteasomes during prophase can be considered an additional mechanism that contributes to cyclin B accumulation in the nucleus, allowing the cdk–cyclin B complex to reach its higher level of activity.

We have shown the dynamic association between proteasomes and chromosomal regions actively engaged in DNA replication during S phase (Figs. 8, 9). DNA synthesis during S phase begins by the formation of pre-RC complexes at replication origins. These processes can be described as the cooperation between several matchmaker proteins, allowing the final loading of DNA polymerase (Tye, 1999). What could be the function of the proteasome association with regions of chromatin engaged in active replication? The obvious answer is that proteasome degrades some proteins, permitting the remodeling of the protein complexes involved in the firing of replication origins. In *Saccharomyces cerevisiae*, one of such proteolytic events is the degradation of Cdc6p (Piatti et al., 1995), while in mammals the Cdc6p homologue is not degraded, but rather is transported out of the nucleus (Fujita et al., 1999). Another protein candidate is the newly identified protein Cdt1 of *S. pombe*, and its homologues in *Xenopus laevis* and mammals, which cooperate with Cdc6 to promote DNA replication (Nishitani et al., 2000; Maiorano et al., 2000) and are removed by proteolysis at the initiation of DNA synthesis. Nevertheless, we suggest another possible function of proteasomes in DNA replication, and probably in other phases of the cell cycle as well. Although the ATPase subunits of the base of the 19S complex are believed to drive protein unfolding before degradation, the 19S complex alone or in association with the 20S proteasome (26S proteasome complex) also function as chaperones (Braun et al., 1999; Strickland et al., 2000). The role of the proteasome in DNA transactions has some direct experimental support. It has been shown that the yeast 19S complex, but not the proteolytic activity of the 20S catalytic core, participates in nucleotide excision repair in yeast (Russell et al., 1999; Gillette et al., 2001). From a functional point of view, six subunits of the base of the 19S complex (Voges et al., 1999), and the proteins involved in the formation of pre-RC complexes (also in prokaryotes) belong to the AAA family of ATPases (Lee and Bell, 2000). In prokaryotes, the ClpA/XP protease (functional homologues of proteasome) also serves a dual function. ClpAX/P behaves as a chaperone (ClpA and ClpX are also members of the AAA family of ATPases), or as a proteases (ClpA and ClpX use ATP hydrolysis to unfold substrates to be degraded by the ClpP catalytic core). Both activities of ClpA/XP have been shown to be important for DNA replication in prokaryotes (Wawrzynow et al., 1996; Jones et al., 1998; Jenal and Fuchs, 1998). As a consequence, we suggest that proteasome complexes can serve a dual function in DNA replication, contributing through the 19S complex (alone or in association with the 20S catalytic core) to chaperon certain proteins required for DNA synthesis and producing the remodeling of those complexes by selective degradation of some of the proteins involved.

In conclusion, we demonstrate the location of the proteasomes in the mammalian cell during the major events of cell cycle, S and M phase. Even if unimpeded motion in the nucleus and cytoplasm of proteasomes and their putative substrates determines the rate of productive collisions, it is clear that the steady-state concentration of proteasomes shows preferential subcellular localization within the cell that changes during the cell cycle.

ACKNOWLEDGMENTS

This work was supported by Comisión Interministerial de Ciencia y Tecnología (SAF99-0056), Comunidad Autónoma de Madrid (CAM), and Fundación La Caixa (to J.G.C.) and by Fondo de Investigaciones Sanitarias (00/0947), Fundación Marqués de Valdecilla (to M.T.B.

and R.F.). I.M. is the recipient of a predoctoral fellowship from Fundación La Caixa.

REFERENCES

Amsterdam A, Pitzer F, Baumeister W. 1993. Changes in intracellular localization of proteasomes in immortalized ovarian granulosa cells during mitosis associated with a role in cell cycle control. Proc Natl Acad Sci U S A 90:99–103.

Arcangeletti C, Sutterlin R, Aebi U, De Conto F, Missorini S, Chezzi C, Scherrer K. 1997. Visualization of prosomes (MCP-proteasomes), intermediate filament and actin networks by "instantaneous fixation" preserving the cytoskeleton. J Struct Biol 119:35–58.

Arcangeletti C, De Conto F, Sutterlin R, Pinardi F, Missorini S, Geraud G, Aebi U, Chezzi C, Scherrer K. 2000. Specific types of prosomes distribute differentially between intermediate and actin filaments in epithelial, fibroblastic and muscle cells. Eur J Cell Biol 79:423–437.

Arizti P, Arribas J, Castaño JG. 1993. Modulation of the multicatalytic proteinase complex by lipids, interconversion and proteolytic processing. Enzyme Protein 47:285–295.

Arribas J, Arizti P, Castaño JG. 1994. Antibodies against the C2 COOH-terminal region discriminate the active and latent forms of the multicatalytic proteinase complex. J Biol Chem 269:12858–12864.

Bochtler M, Ditzel L, Groll M, Hartmann C, Huber R. 1999. The proteasome. Annu Rev Biophys Biomol Struct 28:295–317.

Braun BC, Glickman M, Kraft R, Dahlmann B, Kloetzel PM, Finley D, Schmidt M. 1999. The base of the proteasome regulatory particle exhibits chaperone-like activity. Nat Cell Biol 1:221–226.

Brockes JP, Fields KL, Raff MC. 1979. Studies on cultured rat Schwann cells. I. Establishment of purified populations from cultures of peripheral nerve. Brain Res 165:105–118.

Brooks P, Fuertes G, Murray RZ, Bose S, Knecht E, Rechsteiner MC, Hendil KB, Tanaka K, Dyson J, Rivett J. 2000. Subcellular localization of proteasomes and their regulatory complexes in mammalian cells. Biochem J 346:155–161.

Cerutti L, Simanis V. 2000. Controlling the end of the cell cycle. Curr Opin Genet Dev 10:65–69.

Chao DS, Hay JC, Winnick S, Prekeris R, Klumperman J, Scheller RH. 1999. SNARE membrane trafficking dynamics in vivo. J Cell Biol 144:869–881.

Clute P, Pines J. 1999. Temporal and spatial control of cyclin B1 destruction in metaphase. Nat Cell Biol 1:82–87.

Cooper JA, Schafer DA. 2000. Control of actin assembly and disassembly at filament ends. Curr Opin Cell Biol 12:97–103.

Donaldson AD, Blow JJ. 1999. The regulation of replication origin activation. Curr Opin Genet Dev 9:62–68.

Fabunmi RP, Wigley WC, Thomas PJ, DeMartino GN. 2000. Activity and regulation of the centrosome-associated proteasome. J Biol Chem 275:409–413.

Farmaki T, Ponnambalam S, Prescott AR, Clausen H, Tang BL, Hong W, Lucocq JM. 1999. Forward and retrograde trafficking in mitotic animal cells. ER-Golgi transport arrest restricts protein export from the ER into COPII-coated structures. J Cell Sci 112:589–600.

Ferdous A, Gonzalez F, Sun L, Kodadek T, Johnston SA. 2001. The 19S regulatory particle of the proteasome is required for efficient transcription elongation by RNA polymerase II. Mol Cell 7:981–991.

Foucrier J, Bassaglia Y, Grand MC, Rothen B, Perriard JC, Scherrer K. 2001. Prosomes form sarcomere-like banding patterns in skeletal, cardiac, and smooth muscle cells. Exp Cell Res 266:193–200.

Fujita M, Yamada C, Goto H, Yokoyama N, Kuzushima K, Inagaki M, Tsurumi T. 1999. Cell cycle regulation of human CDC6 protein. Intracellular localization, interaction with the human mcm complex, and CDC2 kinase-mediated hyperphosphorylation. J Biol Chem 274:25927–25932.

Gillette TG, Huang W, Russell SJ, Reed SH, Johnston SA, Friedberg EC. 2001. The 19S complex of the proteasome regulates nucleotide excision repair in yeast. Genes Dev 15:1528–1539.

Goldberg JL, Barres BA. 2000. The relationship between neuronal survival and regeneration. Annu Rev Neurosci 23:579–612.

Goode BL, Drubin DG, Barnes G. 2000. Functional cooperation between the microtubule and actin cytoskeletons. Curr Opin Cell Biol 12:63–71.

Hershko A, Ciechanover A. 1998. The ubiquitin system. Annu Rev Biochem 67:425–479.

Hozak P, Jackson DA, Cook PR. 1994. Replication factories and nuclear bodies: the ultrastructural characterization of replication sites during the cell cycle. J Cell Sci 107:2191–2202.

Jenal U, Fuchs T. 1998. An essential protease involved in bacterial cell-cycle control. EMBO J 17:5658–5669.

Johnston JA, Ward CL, Kopito RR. 1998. Aggresomes: a cellular response to misfolded proteins. J Cell Biol 143:1883–1898.

Jones JM, Welty DJ, Nakai H. 1998. Versatile action of *Escherichia coli* ClpXP as protease or molecular chaperone for bacteriophage Mu transposition. J Biol Chem 273:459–465.

Jorgensen PM, Brundell E, Starborg M, Hoog C. 1998. A subunit of the anaphase-promoting complex is a centromere-associated protein in mammalian cells. Mol Cell Biol 18:468–476.

Kurasawa Y, Todokoro K. 1999. Identification of human APC10/Doc1 as a subunit of anaphase promoting complex. Oncogene 18:5131–5137.

LaBaer J, Garrett MD, Stevenson LF, Slingerland JM, Sandhu C, Chou HS, Fattaey A, Harlow E. 1997. New functional activities for the p21 family of CDK inhibitors. Genes Dev 11:847–862.

Lee DG, Bell SP. 2000. ATPase switches controlling DNA replication initiation. Curr Opin Cell Biol 12:280–285.

Maiorano D, Moreau J, Mechali M. 2000. XCDT1 is required for the assembly of pre-replicative complexes in *Xenopus laevis*. Nature 404:622–625.

Mazzotti G, Gobbi P, Manzoli L, Falconi M. 1998. Nuclear morphology during the S phase. Microsc Res Tech 40:418–431.

Mengual E, Arizti P, Rodrigo J, Gimenezamaya JM, Castaño JG. 1996. Immunohistochemical distribution and electron microscopic subcellular localization of the proteasome in the rat CNS. J Neurosci 16:6331–6341.

Mirsky R, Jessen KR. 1999. The neurobiology of Schwann cells. Brain Pathol 9:293–311.

Morgan L, Jessen KR, Mirsky R. 1991. The effects of cAMP on differentiation of cultured Schwann cells: progression from an early phenotype ($O4^+$) to a myelin phenotype ($P0^+$, $GFAP^-$, $N\text{-}CAM^-$, $NGF\text{-}receptor^-$) depends on growth inhibition. J Cell Biol 112:457–467.

Muller D, Thieke K, Burgin A, Dickmanns A, Eilers M. 2000. Cyclin E-mediated elimination of p27 requires its interaction with the nuclear pore-associated protein mNPAP60. EMBO J 19:2168–2180.

Nishitani H, Lygerou Z, Nishimoto T, Nurse P. 2000. The Cdt1 protein is required to license DNA for replication in fission yeast. Nature 404:625–628.

Notterpek L, Ryan MC, Tobler AR, Shooter EM. 1999. PMP22 accumulation in aggresomes: implications for CMT1A pathology. Neurobiol Dis 6:450–460.

Nurse P. 2000. A long twentieth century of the cell cycle and beyond. Cell 100:71–78.

Olink-Coux M, Arcangeletti C, Pinardi F, Minisini R, Huesca M, Chezzi C, Scherrer K. 1994. Cytolocation of prosome antigens on intermediate filament subnetworks of cytokeratin, vimentin and desmin type. J Cell Sci 107:353–366.

Palmer A, Mason GG, Paramio JM, Knecht E, Rivett AJ. 1994. Changes in proteasome localization during the cell cycle. Eur J Cell Biol 64:163–175.

Palmer A, Rivett AJ, Thomson S, Hendil KB, Butcher GW, Fuertes G, Knecht E . 1996. Subpopulations of proteasomes in rat liver nuclei, microsomes and cytosol. Biochem J 316:401–407.

Phair RD, Misteli T. 2000. High mobility of proteins in the mammalian cell nucleus. Nature 404:604–609.

Piatti S, Lengauer C, Nasmyth K. 1995. Cdc6 is an unstable protein whose de novo synthesis in G1 is important for the onset of S phase and for preventing a "reductional" anaphase in the budding yeast *Saccharomyces cerevisiae*. EMBO J 14:3788–3799.

Reits EAJ, Benham AM, Plougastel B, Neefjes J, Trowsdale J. 1997. Dynamics of proteasome distribution in living cells. EMBO J 16: 6087–6094.

Rivett AJ, Palmer A, Knecht E. 1992. Electron microscopic localization of the multicatalytic proteinase complex in rat liver and in cultured cells . J Histochem Cytochem 40:1165–1172.

Rodriguez-Vilarino S, Arribas J, Arizti P, Castaño JG. 2000. Proteolytic processing and assembly of the C5 subunit into the proteasome complex. J Biol Chem 275:6592–6599.

Russell SJ, Reed SH, Huang W, Friedberg EC, Johnston SA. 1999. The 19S regulatory complex of the proteasome functions independently of proteolysis in nucleotide excision repair. Mol Cell 3:687–695.

Strickland E, Hakala K, Thomas PJ, DeMartino GN. 2000. Recognition of misfolding proteins by PA700, the regulatory subcomplex of the 26 S proteasome. J Biol Chem 275:5565–5572.

Tanahashi N, Murakami Y, Minami Y, Shimbara N, Hendil KB, Tanaka K. 2000. Hybrid proteasomes. Induction by interferon-gamma and contribution to ATP-dependent proteolysis. J Biol Chem 275:14336–14345.

Tye BK. 1999. MCM proteins in DNA replication. Annu Rev Biochem 68:649–686.

Tyers M, Jorgensen P. 2000. Proteolysis and the cell cycle: with this RING I do thee destroy. Curr Opin Genet Dev 10:54–64.
Voges D, Zwickl P, Baumeister W. 1999. The 26S proteasome: a molecular machine designed for controlled proteolysis. Annu Rev Biochem 68:1015–1068.
Wawrzynow A, Banecki B, Zylicz M. 1996. The Clp ATPases define a novel class of molecular chaperones. Mol Microbiol 21:895–899.
Wei X, Samarabandu J, Devdhar RS, Siegel AJ, Acharya R, Berezney R. 1998. Segregation of transcription and replication sites into higher order domains. Science 281:1502–1506.
Weiner JA, Fukushima N, Contos JJ, Scherer SS, Chun J. 2001. Regulation of Schwann cell morphology and adhesion by receptor-mediated lysophosphatidic acid signaling. J Neurosci 21:7069–7078.
Wigley WC, Fabunmi RP, Lee MG, Marino CR, Muallem S, DeMartino GN, Thomas PJ. 1999. Dynamic association of proteasomal machinery with the centrosome. J Cell Biol 145:481–490.
Wojcik C, Paweletz N, Schroeter D. 1995. Localization of proteasomal antigens during different phases of the cell cycle in HeLa cells. Eur J Cell Biol 68:191–198.
Yang Y, Fruh K, Ahn K, Peterson PA. 1995. In vivo assembly of the proteasomal complexes, implications for antigen processing. J Biol Chem 270:27687–27694.
Zaal KJ, Smith CL, Polishchuk RS, Altan N, Cole NB, Ellenberg J, Hirschberg K, Presley JF, Roberts TH, Siggia E, Phair RD, Lippincott-Schwartz J. 1999. Golgi membranes are absorbed into and reemerge from the ER during mitosis. Cell 99:589–601.